Available online at www.sciencedirect.com
ScienceDirect
Cement and Concrete Research 37 (2007) 796–804
Cement and Concrete Research

Extracting the performance predictors of Enhanced Porosity Concretes from electrical conductivity spectra

Narayanan Neithalath *

Department of Civil and Environmental Engineering, Clarkson University, Potsdam, NY 13699, USA

Received 24 January 2006; accepted 13 February 2007

Abstract

This paper discusses the application of an analytical model of the dielectric spectrum of Enhanced Porosity Concretes (EPC, or pervious concretes) to predict its porosity and effective conductivity. While porosity is the dominant material parameter that dictates the performance characteristics (acoustic absorption and hydraulic conductivity) of EPC, effective conductivity has been shown to be an important parameter in the non-destructive estimation of performance. The porosities of the EPC specimens were measured using a volumetric method and an image analysis method. The effective conductivities were calculated from the bulk resistances of the samples obtained from Nyquist plots. The fits of the model to the conductivity spectra were used to extract the values of porosity and effective conductivity. The measured and predicted values of porosities and effective conductivities show good correlation. The frequency dependence of the dielectric spectra as well as the advantages of using a conductivity spectrum as opposed to a dielectric constant spectrum is outlined. The need to use effective conductivity rather than conductivity at any frequency is also brought out. It is shown that a single electrical conductivity spectrum could be used to predict the parameters that best describe the performance characteristics of EPC.

Keywords: Electrical properties; Permeability; Porosity; Conductivity spectra; Acoustic absorption; Enhanced Porosity (pervious) Concrete

1. Introduction

Enhanced Porosity Concrete (EPC), also known as pervious concrete, is a special class of concrete proportioned by using gap graded coarse aggregates, very little or no fine aggregates, and a low water-to-cement ratio. This facilitates the development of a network of interconnected pores in the system. Such a pore structure makes the percolation of water through an EPC layer easy, thus recharging the ground water and conserving water resources. This property has made the use of EPC a sustainable alternative to impervious areas in regions of moderate to high rainfall intensity. Pervious surfaces in parking lots are believed to help infiltration and cleansing of storm water, thereby reducing the adverse environmental impact of impervious parking areas [1,2]. The other notable advantage of EPC is its ability to minimize the tire–pavement interaction noise which has become a significant environmental issue [3,4]. This is achieved by a combination of reduction in noise generation (by minimizing air pumping, which is the pumping of air in and out of the tread blocks of the tire) and increased absorption of acoustic energy (by the tortuous macropore network in the system) [3].

The hydraulic and acoustic properties of EPC depend heavily on its pore structure (porosity, pore sizes, and pore connectivity) [5,6]. Porosity is the most easily quantifiable pore structure feature of any porous material. For EPC to be effective in rapidly draining surface water, a total porosity of 20% or more is needed whereas for sound absorption, it has been stated that 15–25% accessible porosity (pore volume accessible to the incident sound waves) is necessary [7–9].

Using electrical impedance studies [5], it has been shown that the acoustic absorption coefficient (measure of a material's capacity to absorb the incident sound energy) of EPC is linearly related to the pore connectivity factor (β_p), which is a function of the porosity (ϕ), and modified normalized conductivity σ^*_{norm} as follows:

$$\beta_p = \frac{\sigma^*_{norm}}{\phi} \quad (1)$$

* Tel.: +1 315 268 1261; fax: +1 315 268 7985.
E-mail address: nneithal@clarkson.edu.

0008-8846/$ - see front matter © 2007 Elsevier Ltd. All rights reserved.
doi:10.1016/j.cemconres.2007.02.018

where

$$\sigma^*_{\text{norm}} = \frac{[\sigma_{\text{eff}} - \sigma_{\text{solid}}(1-\phi)]}{\sigma_{\text{pore}}} \tag{2}$$

σ_{eff} is the effective conductivity, σ_{pore} is the conductivity of the electrolyte filling the large pores in the material, and σ_{solid} is the conductivity of the solid phase (the matrix that coats the aggregates).

Similarly, the intrinsic permeability, k, which is related to hydraulic conductivity K ($K = k\frac{\rho g}{\mu}$; ρ and μ are respectively the density and dynamic viscosity of the fluid, g is the acceleration due to gravity) of EPC has been found to adhere to a modified version of Kozeny–Carman equation [10,11,5]:

$$k \propto \left[\sigma^*_{\text{norm}}\right]^2 \left(\frac{\phi}{(1-\phi)^2}\right). \tag{3}$$

It can be noticed from Eqs. (1) and (3) that the transport characteristics of both acoustic waves and water in EPC are dependent on the material porosity and the effective conductivity (through the normalized conductivity). Hence, the determination of these parameters is essential to ensure performance adequacy of EPC in water transport and acoustic absorption.

This paper presents a methodology based on an analytical model of a two-component composite [12,13] to extract the porosity and effective electrical conductivity of EPC specimens from dielectric dispersion measurements. Though the dispersion of both dielectric permittivity as well as electrical conductivity with frequency can be used to determine porosity [13–16], this paper primarily makes use of the electrical conductivity spectra because of (i) large enhancement in dielectric constant at low frequencies [14,16–18], and (ii) the capability of this model to predict effective conductivity of the material also in addition to porosity.

2. Analytical representation of the dielectric behavior of EPC

The dielectric behavior of composite materials is described to varying degrees of accuracy by the mixing models [16,19–25], depending on the range of frequencies selected. One approach to extract the pore structure features of porous materials is based on the theory of dielectric dispersion (dispersion of permittivity and conductivity) of granular materials [14,15,26,27]. In the frequency range from Hz to MHz, the conductivity σ increases with increasing frequency, whereas the effective dielectric constant ε (ratio of dielectric permittivity ε_r of the material to that of vacuum ε_0) increases with decreasing frequency and stabilizes at an asymptotic value at very high frequencies [13,26,28]. A modified analytical form for the Bergman dielectric response of two phase composites [12] is used in this paper to predict the frequency dependent dielectric properties of EPC. The major feature of this model that makes it attractive for EPC is an implicit hypothesis of small grain contact area, i.e., it is assumed that the contact area with the neighboring grains is small compared to the grain area.

The complex dielectric constant $\varepsilon(\omega)$ of an isotropic two-component composite consisting of an insulating solid phase and a pore phase filled with a conducting fluid, as a function of angular frequency ω, is given by:

$$\varepsilon(\omega) = \varepsilon'(\omega) - i\frac{\sigma(\omega)}{\omega} \tag{4}$$

$\sigma(\omega)$ and $\varepsilon'(\omega)$ are the frequency dependent conductivity and real part of the dielectric constant respectively of the composite. These quantities are related to the conductivity and dielectric constants of the pore and solid phases.

A complete description of the model development can be found in [12] where it is stated that $\left(\frac{\varepsilon(\omega)}{\varepsilon_{\text{solid}}(\omega)}\right)$ is a function of $s(\omega)$; where $s(\omega) = \frac{1}{1-\frac{\varepsilon_{\text{pore}}(\omega)}{\varepsilon_{\text{solid}}(\omega)}}$. $\varepsilon_{\text{solid}}(\omega)$ is the dielectric constant of the solid phase, and $\varepsilon_{\text{pore}}(\omega)$, that of the pore phase filled with a fluid. In a composite where $\varepsilon_{\text{pore}} \to 0$ (mostly solid phase), $s \to 1$, and therefore $f(s) = f(1) \leq 1$. For other values of $\varepsilon_{\text{pore}}$, $f(s)$ can be represented using a singular integral equation of the first kind, and the solutions represented as:

$$\varepsilon'(\omega) = \varepsilon^{1-b}_{\text{solid}} \left(\frac{\sigma_{\text{pore}}}{\varepsilon_0}\right)^b \left[\frac{C}{2\sin(b\pi/2)}\right] \omega^{-b} \tag{5}$$

$$\sigma(\omega) = \sigma_{\text{pore}} \left[A + \left(\frac{\varepsilon_{\text{solid}}\varepsilon_0\omega}{\sigma_{\text{pore}}}\right)^{1-b}\right] \tag{6}$$

A, b, and C are the model parameters, and ε_0, the permittivity of free space (8.884×10^{-12} F/m).

For a composite in which one phase is completely insulating, the parameter A can be given an Archie's law equivalent form as:

$$A = \frac{\sigma_{\text{eff}}}{\sigma_{\text{pore}}} = \phi^m \Rightarrow \sigma_{\text{eff}} = \sigma_{\text{pore}}\phi^m \tag{7}$$

But it has been previously shown that EPC does not obey single conducting phase Archie's law, and a modified version has been proposed, accounting for the conductivity and volume fractions of the solid matrix phase also [5], as:

$$\sigma_{\text{eff}} = \sigma_{\text{pore}}\phi^m + \sigma_{\text{solid}}\phi^{m'}_{\text{solid}} \tag{8}$$

σ_{solid} is the conductivity of solid phase (in a saturated condition), and ϕ_{solid} is its volume fraction, which is equal to $(1-\phi)$. The exponents m and m' represent the degree of connectivity of the pore and solid phases respectively; a lower value indicating better connectivity [19]. It was observed that, for EPC, the term m' is very small (0.03–0.10) [5], rendering the value of $\phi^{m'}_{\text{solid}}$ close to 1.0. Hence, the modified Archie's law can be simplified to:

$$\sigma_{\text{eff}} = \sigma_{\text{pore}}\phi^m + \sigma_{\text{solid}} \tag{9}$$

Table 1
Experimentally determined and predicted values of the parameters

Mixture ID	Measured porosity			Predicted porosity (using Eq. (11) to fit the conductivity spectra)			Effective conductivity σ_{eff}, S/m			
Maximum aggregate sizes (% of each size by weight)	Volumetric method	Image analysis	Avg. [a]	σ_{pore}=1.77 S/m	σ_{pore}=4.4 S/m	Avg. [a]	σ_{pore}=1.77 S/m		σ_{pore}=4.4 S/m	
							Meas [b]	Pred [c]	Meas [b]	Pred [c]
4.75 mm (100%)	0.207	0.214	0.210	0.204	0.210	0.207	0.037	0.044	0.094	0.091
4.75 mm (75%) 9.5 mm (25%)	0.208	0.305	0.257	0.231	0.290	0.261	0.042	0.043	0.109	0.108
4.75 mm (50%) 9.5 mm (50%)	0.247	0.260	0.254	0.272	0.281	0.277	0.046	0.066	0.141	0.150
4.75 mm (25%) 9.5 mm (75%)	0.225	0.276	0.250	0.286	0.271	0.279	0.058	0.064	0.189	0.192
9.5 mm (100%)	0.206	0.203	0.205	0.190	0.194	0.192	0.035	0.036	0.083	0.079
12.5 mm (100%)	0.193	0.237	0.215	0.145	0.155	0.150	0.009	0.005	0.038	0.032
4.75 mm (25%) 12.5 mm (75%)	0.174	0.244	0.209	0.160	0.280	0.220	0.009	0.008	0.077	0.074
9.5 mm (97.5%), sand (2.5%)	0.187	0.189	0.188	–	0.201	0.201	–		0.043	0.038
9.5 mm (95%), sand (5%)	0.176	0.212	0.194	–	0.180	0.180	–		0.033	0.029

[a] Average.
[b] Measured effective conductivity (calculated from bulk resistance of the Nyquist plots).
[c] Predicted effective conductivity from the fit of Eq. (11) to the experimental data.

The parameter A, which is equal to ϕ^m could then be represented as:

$$A = \phi^m = \frac{\sigma_{eff} - \sigma_{solid}}{\sigma_{pore}} \tag{10}$$

The equation for conductivity as a function of frequency, Eq. (6), then becomes:

$$\sigma(\omega) = \sigma_{pore}\left[\left(\frac{\sigma_{eff} - \sigma_{solid}}{\sigma_{pore}}\right) + \left(\frac{\varepsilon_{solid}\varepsilon_0\omega}{\sigma_{pore}}\right)^{1-b}\right] \tag{11}$$

where

$$b = 1 - \left(\frac{\phi(1-\phi)}{2\phi - \left[\frac{\sigma_{eff} - \sigma_{solid}}{\sigma_{pore}}\right](3-\phi)}\right) \tag{12}$$

The parameter b is a function of the porosity of the material, the effective conductivity, and the conductivities of the pore and solid phase. The solid conductivities of the EPC specimens can be obtained from Eq. (9) by determining the effective conductivities at two known electrolyte conductivities so that simultaneous equations in σ_{solid} and m could be solved. Fitting Eq. (11) to the experimentally determined conductivity spectra facilitates the determination of the constant b and the effective conductivity. The porosity ϕ can then be extracted from Eq. (12).

3. Experimental program

3.1. Mixture proportions and specimen preparation

The mixture proportions used in this study were adopted from a larger experimental program that was designed to determine the mechanical, acoustic, and hydraulic properties of EPC [5,9]. The mixtures were made using single sized aggregates (limestone aggregates with a specific gravity 2.72) and their binary blends. The single sized aggregates had maximum sizes of 4.75 mm (passing 4.75 mm, retained on 2.36 mm sieve), 9.5 mm (passing 9.5 mm, retained on 4.75 mm sieve), or 12.5 mm (passing 12.5 mm, retained on 9.5 mm sieve). The binary blends were prepared by replacing 25, 50, and 75% by weight of the larger aggregates with smaller aggregates. One series of mixtures had 2.5% and 5% of 9.5 mm maximum size aggregates replaced by river sand. The water–cement ratio of all mixtures was kept constant at 0.33. The cement content was adjusted so that there was no residual paste clogging the pore space, and an aggregate–cement ratio of 5.5 to 5.7 ensured it. The mixtures were prepared using a laboratory mixer in accordance with ASTM C 192, cast in 150 × 150 × 700 mm molds, and consolidated using external vibration. Cylinders (95 mm diameter) that were cored from the above beam specimens were used for the tests described in this paper.

3.2. Measurement of porosity

The porosity of EPC was determined using a volumetric method and an image analysis procedure. For the volumetric method, the cylindrical specimens (95 mm in diameter and 150 mm long) that were cored from beams were immersed in water for 24 h to saturate the pores in the matrix. After removal from water, the sample was enclosed in a latex membrane and the bottom of the specimen was sealed to a stainless steel plate using silicone sealant. The mass of this system was measured. Water was added to the top of the sample until it was filled, which indicated that all the interconnected pores were saturated. The volume of water needed to fill the specimen, expressed as a percentage of the total volume of the specimen, is reported as the total porosity. In the image analysis method, the EPC specimen was impregnated with a low viscosity epoxy, and sectioned at different depths. The surface of each section was scanned using a flat bed scanner, and an image conditioning and feature measurement procedure using a commercial software (ImagePro Plus©) was employed to estimate the fractional area of pores. The average of fractional pore areas of all sections is taken as the specimen porosity [9]. Both these methods resulted in comparable values of porosity as shown in Table 1 (except for one mixture where the values are vastly different and therefore

omitted in the forthcoming analysis). The differences in porosity between the two methods of measurement are attributed to the volume and area concepts employed in porosity determination [5].

3.3. Measurement of electrical impedance spectra of EPC

The use of electrical impedance spectroscopy (EIS) as a characterization tool in the study of cementitious materials has been well documented [17,18,29–31]. EIS measurements were conducted in this study using a Solartron 1260™ Impedance/Gain-Phase analyzer that was interfaced with a personal computer for data acquisition. The cylindrical specimen was enclosed in a latex membrane and the bottom sealed to a stainless steel plate electrode using silicone sealant, with a piece of porous foam in between the specimen and the plate electrode to ensure proper electrical contact. After the specimen was saturated with the electrolyte, another stainless steel plate with a small acrylic dyke was placed at the top of the specimen, with a piece of porous foam in between. The impedance measurements were made over the frequency range of 10 MHz or 1 MHz to 10 Hz or 1 Hz using a 250 mV AC signal.

The Nyquist plots represent the relationship between the real or resistive [$Z'(\omega)$] and imaginary or reactive [$Z''(\omega)$] components of the impedance given by:

$$Z(\omega) = Z'(\omega) - iZ''(\omega) \tag{13}$$

A typical Nyquist plot is shown in Fig. 1. From the measured electrical impedance spectrum, the conductivity spectrum can be obtained from:

$$\sigma(\omega) = \frac{l}{|Z(\omega)|A_e} \tag{14}$$

where $|Z(\omega)|$ is the absolute value of the impedance, l is the spacing between the electrodes and A_e is the electrode cross-sectional area. Substituting the bulk resistance of the sample R_b (the value of Z' when Z'' is minimum, which is the intersection

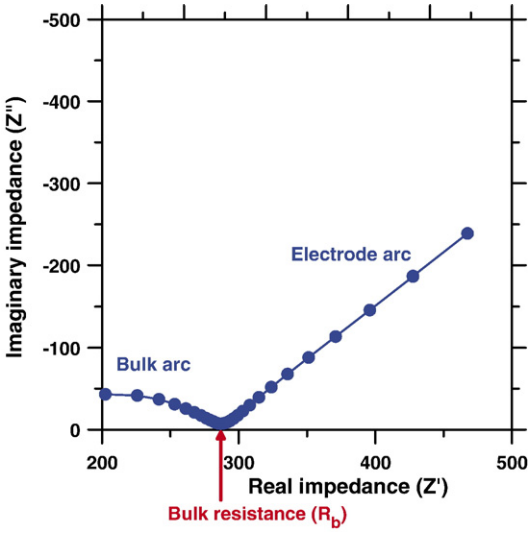

Fig. 1. A typical Nyquist plot for an EPC mixture.

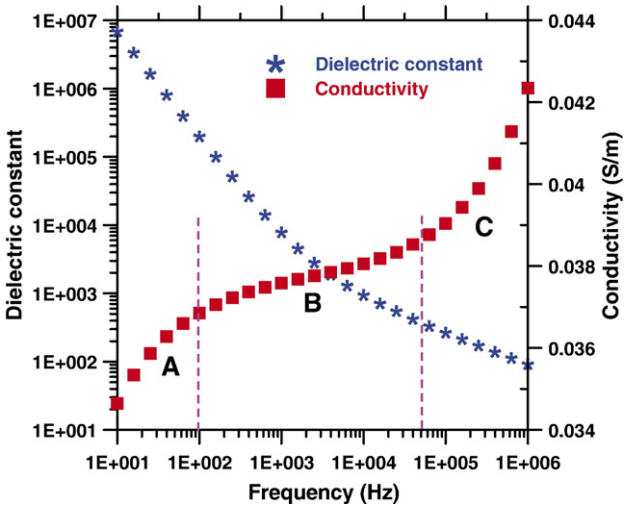

Fig. 2. Frequency dependence of dielectric constant and conductivity (depicted for EPC with 9.5 mm max. size aggregates saturated with 1% NaCl solution).

of the bulk arc and the electrode arc in Fig. 1) for $Z(\omega)$ in Eq. (14) gives the effective conductivity of the specimen σ_{eff}. The frequency corresponding to the bulk resistance R_b is the critical frequency (f_{crit}).

The electrolytes used in this study were NaCl solutions of varying concentrations (1%, 3%, and 10%). The impedance measurements were carried out in the order of increasing ionic strength of the electrolyte. The electrolyte conductivities were calculated from the following empirical equation [12]:

$$\sigma_{pore} = \left[0.0123 + \frac{3647.5}{1000(X)^{0.955}}\right]^{-1} \text{S/m} \tag{15}$$

where X is the salinity in kilo parts per million (kppm). The values of σ_{pore} were found to be 1.77 S/m, 4.4 S/m, and 13.2 S/m for 1%, 3%, and 10% NaCl solutions respectively.

The complex dielectric constant (ε) is determined from the following relationship between impedance and intrinsic electrical properties for a lossy dielectric material placed between a pair of parallel plate electrodes.

$$Z(\omega) = \frac{1}{(i\omega\varepsilon_0\varepsilon)(A_e/l)} \tag{16}$$

4. Results, analysis, and discussions

4.1. Frequency dependence of measured dielectric constant and conductivity

The real part of the dielectric constant (ε') obtained from the impedance data using Eq. (16) as well as the conductivity (σ) from Eq. (14) is dependent on the frequency. In Fig. 2, this dependence is shown for EPC mixture with 9.5 mm maximum size aggregates saturated with 1% NaCl solution in the frequency range of 10 Hz to 1 MHz. The ε' and σ values for all the other EPC specimens investigated in this study also demonstrate a similar frequency dependence. It could be observed that the dielectric constant has remarkably high values at low frequencies.

The common reasons attributed to this behavior are: (a) electrode polarization (Maxwell–Wagner effect) [17,32], (b) dielectric response of the ions at the solid-electrolyte interphase, or (c) significant differences in aspect ratio of particles in the medium [33]. The low frequency dielectric constant values for EPC obtained in this study are in the range reported for brine saturated porous media [34].

The conductivity increases with increasing frequency. The low values of conductivity at lower frequencies (less than approximately 100 Hz, denoted as region A in Fig. 2) are because of the electrode effects. There is a relatively constant conductivity plateau at mid-frequencies (approximately 0.5 kHz to 5 kHz), denoted as region B in Fig. 2. The extent of this plateau zone depends on the porosity, electrolyte conductivity, and the phase geometry of the constituents. The effective conductivity (σ_{eff}) of EPC falls in this plateau zone. At close to MHz frequencies (region C), a rapid increase in conductivity is observed, which can be attributed to two effects: (i) high frequency shunting of dielectric barriers between conductive clusters, resulting in an apparent increase in the effective volume of the conducting phase [32], and (ii) relaxation of the polarization mechanism.

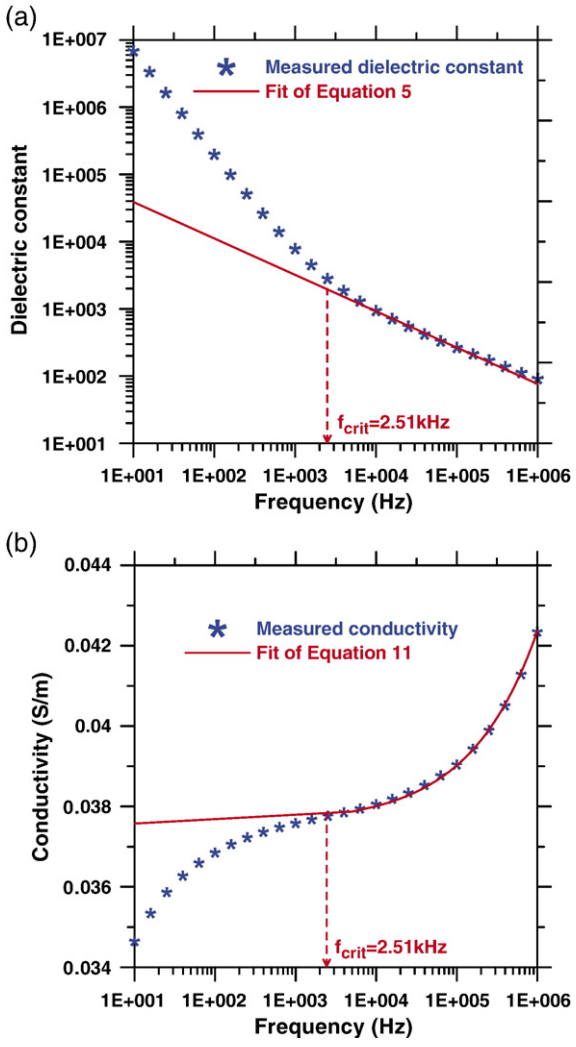

Fig. 3. Experimental values and the corresponding fits for the relationship between frequency and (a) dielectric constant, (b) conductivity (depicted for EPC with 9.5 mm max. size aggregates saturated with 1% NaCl solution).

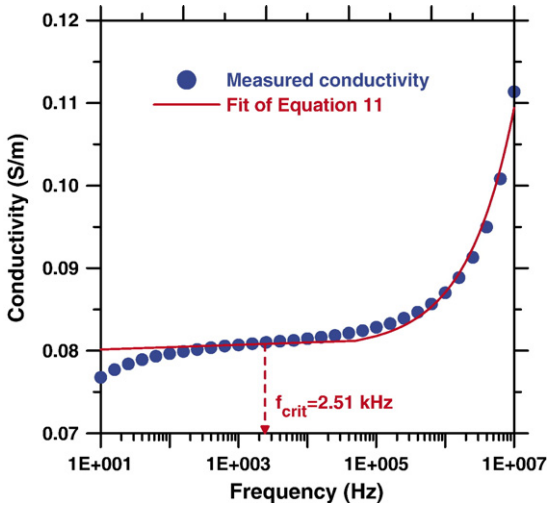

Fig. 4. Conductivity spectrum for EPC with 4.75 mm max. size aggregates saturated with 3% NaCl solution and the fit of Equation to experimental data.

4.2. Comparison of dielectric constant and conductivity spectra to predict porosity

Though $\varepsilon'(\omega)$ and $\sigma(\omega)$ can be used to extract the porosity of EPC [Eqs. (5) and (11)], due to their considerable dispersion explained in the previous section, it is unrealistic to assume that the same model captures all the features of the material at all frequencies. Hence, some cut-off frequency limits are defined in this paper for both dielectric constant and conductivity, above which the analytical model would adequately describe the dielectric response of the material.

Fig. 3(a) and (b) shows the experimentally determined values of $\varepsilon'(\omega)$ and $\sigma(\omega)$ and the fits to the experimental values using Eqs. (5) and (11) as a function of the frequency for the EPC sample made with 9.5 mm maximum size aggregates and saturated with 1% NaCl solution. The fit of Eq. (5) to the measured dielectric constant spectra [Fig. 3(a)] is satisfactory only for higher frequencies. Eq. (5) does not account for the dielectric enhancement occurring at frequencies less than 10 kHz. Similarly, Eq. (11) does not account for the significant reduction in conductivities at frequencies less than 1 kHz [Fig. 3(b)]. However, it could be seen from Fig. 3(a) and (b) that both Eqs. (5) and (11) accurately predict the frequency dependent response of dielectric constant and conductivity respectively at frequencies greater than 2.51 kHz. This happens to be the critical frequency f_{crit} for this sample. Hence these equations could be used to fit the dielectric constant and conductivity data at frequencies higher than f_{crit} in order to predict the porosity and effective conductivity of EPC specimens.

Fig. 4 presents the conductivity spectra and the fit of Eq. (11) for EPC specimens with 4.75 mm maximum size aggregates saturated with 3% NaCl solution. On closer observation of this figure, it can be found that this equation predicts the high frequency response and the mid-frequency plateau region of the conductivity spectra. Hence it seems to be more rational to just

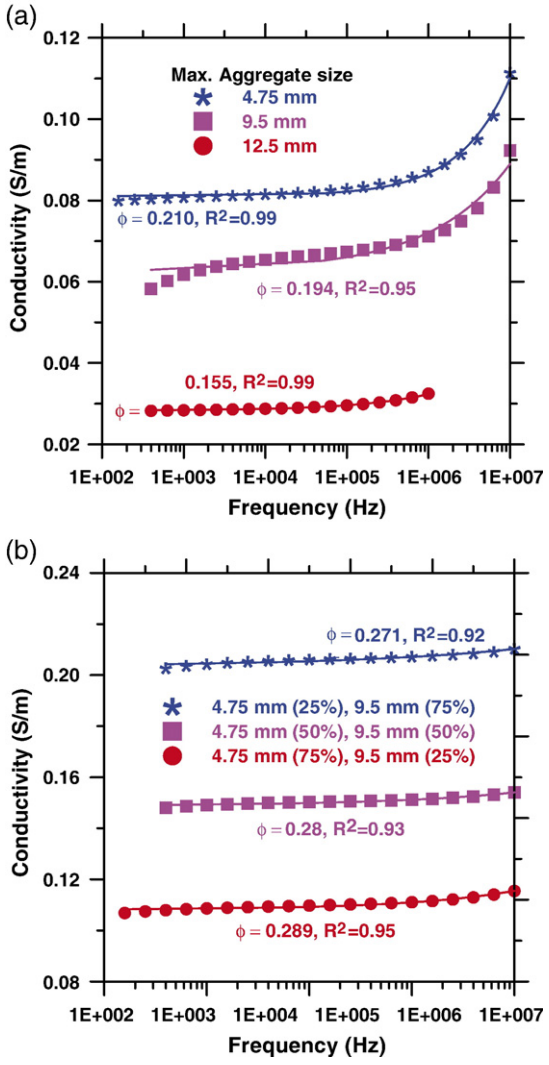

Fig. 5. Conductivity spectra and their fits for (a) single sized EPC mixtures, and (b) blended EPC mixtures, saturated with 3% NaCl solution.

omit the low frequency rising portion of the conductivity spectra (approximately about 100 Hz and lower), rather than ignoring the conductivity at all frequencies lower than f_{crit}, in order to obtain a better fit of the proposed equation to the experimental data. The critical frequency, which happens to be 2.51 kHz in this case also, appears somewhere in the middle of the plateau region.

4.2.1. Advantages of using the conductivity spectra to predict porosity

The parameters of fit to determine ε' from Eq. (5) are the dielectric constant of the solid phase ε_{solid}, and parameters b, and C, whereas to determine σ from Eq. (11), the parameters are ε_{solid}, the effective conductivity of the sample σ_{eff}, and the constant b. The value of ε_{solid} is more significant in the determination of ε' than in that of σ, as might be expected, since Eq. (5) has a multiplicative term $(\varepsilon_{solid})^{1-b}$ whereas in Eq. (11), $\left(\frac{\varepsilon_{solid}\varepsilon_0\omega}{\sigma_{pore}}\right)^{1-b}$ is only an additive term to the normalized effective conductivity $\left(\frac{\sigma_{eff}-\sigma_{solid}}{\sigma_{pore}}\right)$, and the overall term containing ε_{solid} is rather small owing to its multiplication with ε_0. Hence, the equation describing the conductivity spectra is more independent of the dielectric constant of the solid phase than the equation for dielectric constant spectra. This assumes relevance because the term ε_{solid} cannot be considered to be constant irrespective of the electrolyte conductivity. The ionic conductivity of the electrolyte is bound to affect the liquid–solid interfacial polarization phenomena [35], thus influencing the value of ε_{solid} when σ_{pore} is changed. Since this study uses three electrolyte concentrations (1%, 3%, and 10% NaCl), an exact determination of ε_{solid} is not attempted here. The emphasis is on the determination of the constant b which can provide an estimate of the porosity of the system. In addition, the use of the fit for the dielectric constant spectra would need the value of σ_{eff} to be determined beforehand in order to use Eq. (12) (for constant b) to solve for the porosity. The value of σ_{eff} in this case could only be obtained either from the Nyquist plots or from the fit of the conductivity spectra. On the other hand, the fit of Eq. (11) to the conductivity spectra provides the values of both σ_{eff} and b, which can be substituted in Eq. (12) to determine the porosity. Hence the use of conductivity spectrum is found to be ideal to solve the inverse problem of predicting the porosity of EPC.

4.3. Porosity prediction of EPC mixtures

Eq. (11) was fit to the conductivity spectra for frequencies in the plateau region and the high frequency region (regions B and C in Fig. 2). Fig. 5(a) and (b) depicts the fits for the conductivity spectra for EPC with single sized aggregates, and blended aggregates respectively, saturated with 3% NaCl solution. Similar plots were developed for EPC specimens saturated with 1% NaCl also. The porosities obtained from the fits along with the experimentally determined porosities for both the values of σ_{pore} are given in Table 1.

The predicted values of porosity are plotted against measured values as shown in Fig. 6. The average values of porosity determined from the volumetric method and image analysis

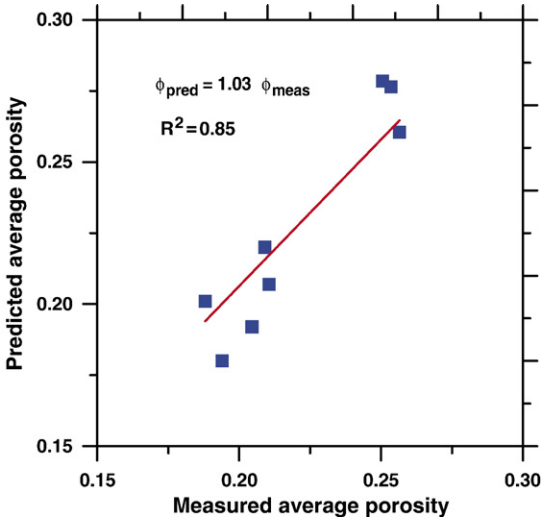

Fig. 6. Relationship between predicted and measured values of porosity.

method are plotted against the average of the porosities calculated from the fits of Eq. (11) to the conductivity spectra of EPC saturated with 1% and 3% NaCl solution. The predicted and measured porosities show reasonably good agreement (R^2 value of 0.85), validating the use of Eq. (11) to solve the inverse problem of determining the porosity from conductivity spectra. The statistical significance of porosity prediction of EPC reported here is comparable to other studies on porosity prediction of water saturated porous glass specimens [15], and dry volcanic rocks [16].

In the data for Fig. 6, the EPC mixture with 12.5 mm maximum size aggregates is not included since the measured and predicted porosities are off by about 30% (Table 1). The reason for such an observation is the following. It can be seen from Fig. 5(a) that EPC with 12.5 mm aggregates has the lowest conductivity even when the measured porosity is fairly close to the other single sized aggregate mixtures. A realistic model for such a specimen will include a cluster of pores that are well connected, but poorly connected to the main pore network in the specimen by a "throat" of negligible conductivity. A detailed analysis has been carried out and reported in an earlier paper [5] to support this argument, which found that the pore connectivity factor (β_p) for this mixture is much lower than other single sized aggregate mixtures (β_p of 0.035 compared to 0.108 for the mixtures with 4.75 mm and 9.5 mm maximum size aggregates). The electrical conductivity spectrum "sees" only the main pore network in the mixture, since the contribution to conductivity from the isolated cluster is negligible, thereby under-predicting the porosity.

4.4. Effective conductivities as determined from the predictive relations

The effective conductivities determined from the fit of Eq. (11) to the conductivity spectra of EPC specimens saturated with 3% NaCl, as well as those calculated from the Nyquist plots are shown in Fig. 7. The fitted and measured values of σ_{eff} are in very good agreement. Table 1 gives the measured and predicted σ_{eff} values for all the EPC specimens investigated, for both the values of σ_{pore}. Eq. (11) could also be solved using σ_{pore} as an additional unknown parameter, thereby making the porosity and effective conductivity prediction independent of the electrolyte conductivity. Since the porosity and effective conductivity values predicted are fairly close to the measured values, it is believed that the predictive equation would also give good estimates of σ_{pore}. This feature of the predictive relation makes it useful as a field tool since the conductivity of the electrolyte in the pores in an EPC system under service is not always easy to measure.

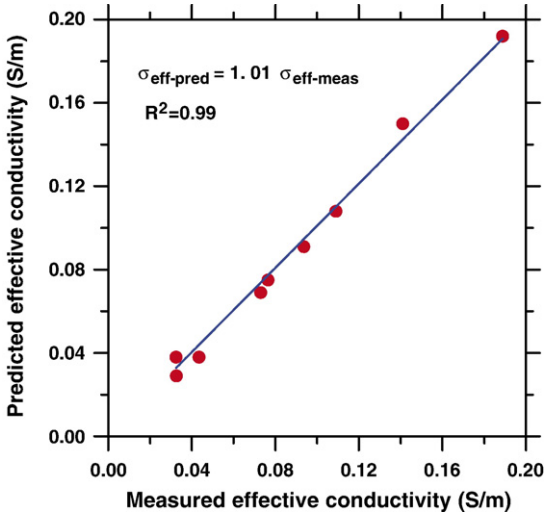

Fig. 7. Relationship between predicted and measured values of effective conductivity (σ_{eff}).

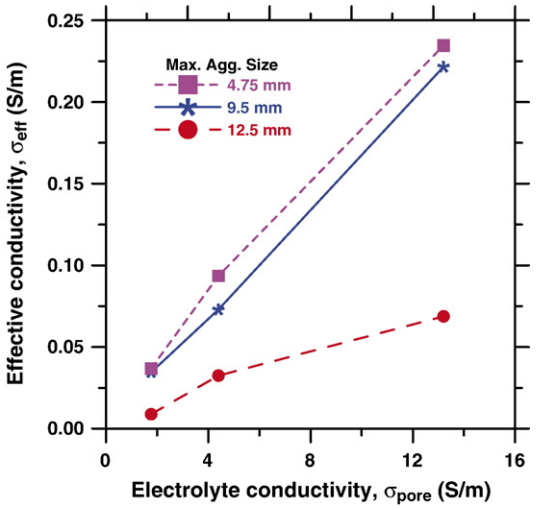

Fig. 8. Effective conductivity (σ_{eff}) as a function of electrolyte conductivity (σ_{pore}) for single sized aggregate EPC mixtures.

4.5. Need to use effective conductivity rather than conductivity at any frequency for performance prediction

The effective conductivities are plotted against the electrolyte conductivities in Fig. 8 for EPC mixtures with single sized

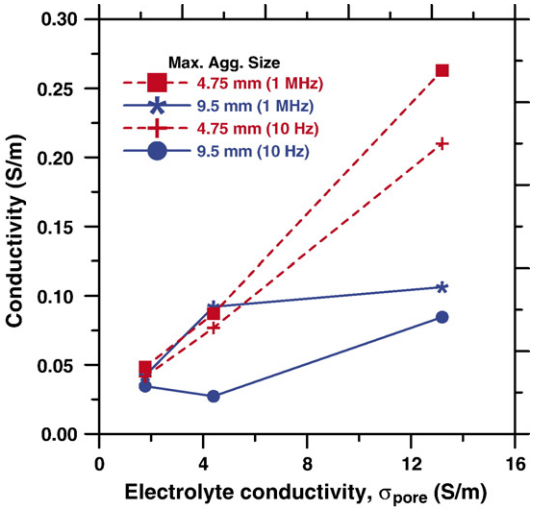

Fig. 9. Relationship between specimen conductivity (σ) and electrolyte conductivity (σ_{pore}) at two different frequencies for single sized aggregate EPC mixtures.

aggregates investigated in this study. All the three single sized aggregate EPC mixtures have similar measured volume porosity values (~0.20 to 0.22). The effective conductivities increase with increase in electrolyte conductivity as expected. Fig. 8 shows that that the increase in effective conductivity of the EPC mixture with 12.5 mm maximum size aggregates is not in line with the trend for the other two mixtures, and the deviation is even more prominent when it is saturated with 10% NaCl solution (σ_{pore} = 13.2 S/m). The reason for such a behavior is that the pore sizes in this mixture are larger than the other two, and the pore connectivity factor is much lower. The effective conductivities of the EPC specimens with 4.75 mm and 9.5 mm maximum size aggregates are very similar, attributable to their similar porosities and pore connectivity factors. It has also been found from a previous study that these two EPC mixtures have very similar acoustic absorption coefficients and hydraulic conductivities [5,9].

Though their performance characteristics are alike, the similarities in electrical response of EPC with 4.75 mm and 9.5 mm maximum size aggregates do not always exist. Fig. 9 relates the electrolyte conductivity to the specimen conductivity at 1 MHz and 10 Hz frequencies for EPC mixtures with these two aggregate sizes. It can be noticed that the conductivities are not similar, especially at higher values of σ_{pore}, contrary to the observations in Fig. 8. If any of these conductivities are used instead of the effective conductivities, the calculated pore connectivity factors [Eq. (1)] would not be similar, and consequently the predicted and measured acoustic absorption coefficients and hydraulic conductivities [Eq. (3)] would differ. Therefore it is imperative that the effective conductivity should be used in the predictive relations for performance. In the methodology described in this paper, it is not required to have prior knowledge of the critical frequency (f_{crit}). The fit of Eq. (11) to the conductivity spectra gives the value of σ_{eff}, which can then be used to calculate the pore connectivity, acoustic absorption coefficient, and hydraulic conductivity. Even though the effective conductivities of two aforementioned mixtures are very similar, the corresponding values of f_{crit} are different, especially at higher values of σ_{pore}. This can be observed from Fig. 10, which relates σ_{eff} to f_{crit} for all the single sized aggregate EPC mixtures. There is no definite frequency or frequency range that is discernible from this figure, in which the effective conductivities of all EPC specimens lie. The same conclusion could be drawn from σ_{eff}–f_{crit} plots of EPC mixtures with aggregate blends of 75% 4.75 mm, 25% 9.5 mm and 50% 9.5 mm, 50% 12.5 mm (not described in this study) which also demonstrate similar effective conductivities.

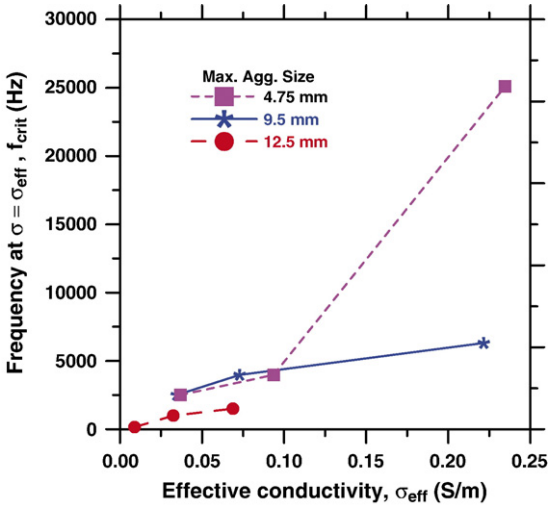

Fig. 10. Relationship between effective conductivity (σ_{eff}) and the critical frequency (f_{crit}) for single sized aggregate EPC mixtures.

5. Conclusions

This paper has dealt with the prediction of porosity and effective conductivity of EPC mixtures from their electrical conductivity spectra. The salient conclusions from this study are listed below:

(i) The analytical form of a modified Bergman equation was found to adequately fit the dielectric constant and conductivity spectra for a certain frequency range. The assumption in the model that the grain contact areas are small compared to the grain areas makes it especially suitable for application to EPC systems.

(ii) The dielectric constant and electrical conductivity spectra show dispersive behavior. The conductivity spectra were used in the paper rather than the dielectric constant spectra to solve the inverse problem of predicting porosity for the following reasons: (a) it gives an estimate of the effective conductivity also of the material, in addition to the porosity, and (b) it is more independent of the dielectric constant of the solid phase. However, with the electrical conductivity spectra also, the Bergman equation does not account for the very low frequency regions because it represents the increasing effects of electrode contribution to the measured conductivity.

(iii) The values of porosity extracted from the fit of the analytical model to the electrical conductivity spectra correlate fairly well with the measured values for the EPC mixtures investigated in this study. The predicted values of effective conductivity also correlate well with the effective conductivity determined from the bulk resistance in Nyquist plots.

(iv) It has been previously found that the transport characteristics of EPC (both hydraulic permeability and acoustic absorption) can be related to its porosity and modified normalized conductivity (a function of effective conductivity). The determination of porosity and effective conductivity from a single equation fitted to the measured conductivity spectra is therefore extremely helpful in determining the performance efficiency of EPC.

(v) The need to use effective conductivity in these predictive equations rather than the conductivity at any frequency has been brought out by illustrating the conductivities of two different EPC mixtures having very similar performance characteristics. The effective conductivities of the investigated EPC mixtures, even when they are similar, do not fall in any specified frequency range.

Acknowledgements

The author wishes to extend his appreciation to Prof. Jan Olek and Prof. Jason Weiss of Purdue University whose guidance was instrumental in leading up to the research reported in this paper.

References

[1] B. Gerharz, Pavements on the base of polymer-modified drainage concrete, Colloids Surf., A Physicochem. Eng. Asp. 152 (1999) 205–209.
[2] J. Yang, G. Jiang, Experimental study on properties of pervious concrete pavement materials, Cem. Concr. Res. 33 (2003) 381–386.
[3] P.M. Nelson, S.M. Phillips, Quieter Road Surfaces, TRL Annual Review, Transportation Research Laboratories, UK, 1994.
[4] Traffic Noises and Road Surfaces: State of the Art, SIRRUS Project, Belgian Road Research Center, Brussels, 2000 March.
[5] N. Neithalath, J. Weiss, J. Olek, Characterizing enhanced porosity concrete using electrical impedance to predict acoustic and hydraulic performance, Cem. Concr. Res. 36 (2006) 2074–2085.
[6] N. Neithalath, A. Marolf, J. Weiss, J. Olek, Modeling the influence of pore structure on the acoustic absorption of Enhanced Porosity Concrete, J. Adv. Concr. Tech. 3 (1) (2005) 29–40.
[7] E. Onstenk, A. Aguado, E. Eickschen, A. Josa, Laboratory Study of Porous Concrete for its Use as Top Layer of Concrete Pavements, Proceedings of the Fifth International Conference on Concrete Pavement and Rehabilitation, Purdue University, Indiana, vol. 2, 1993, pp. 125–139.
[8] Surface properties of concrete roads in accordance with traffic safety and reduction of noise, BRITE/EURAM project BE 3415, November, 1994.
[9] A. Marolf, N. Neithalath, E. Sell, J. Weiss, J. Olek, Influence of aggregate size and gradation on the acoustic absorption of enhanced porosity concrete, ACI Mater. J. 101 (1) (2004) 82–91.
[10] J. Bear, Dynamics of Fluids in Porous Media, Elsevier, New York, 1972.
[11] R.W. Vervoot, S.R. Cattle, Linking hydraulic conductivity and tortuosity parameters to pore space geometry and pore-size distribution, J. Hydrol. 272 (2000) 36–49.
[12] D. Stroud, G.W. Milton, B.R. De, Analytical model for the dielectric response of brine saturated rocks, Phys. Rev., B 34 (8) (1986) 5145–5153.
[13] I. Holwech, B. Nøst, Dielectric dispersion measurements of salt water saturated porous glass, Phys. Rev., B 39 (17) (1989) 12845–12852.
[14] P.N. Sen, C. Scala, M.H. Cohen, A self-similar model for sedimentary rocks with application to dielectric constant of fused glass beads, Geophysics 46 (5) (1981) 781–795.
[15] E. Haslund, B. Nøst, Determination of porosity and formation factor of water saturated porous specimens from dielectric dispersion measurements, Geophysics 63 (1) (1998) 149–153.
[16] A.C. Rust, J.K. Russell, R.J. Knight, Dielectric constant as a predictor of porosity in dry volcanic rocks, J. Volcanol. Geotherm. Res. 91 (1999) 79–96.
[17] W.J. McCarter, G. Starrs, T.M. Chrisp, Immitance spectra for Portland cement/fly ash based binders during early hydration, Cem. Concr. Res. 29 (1999) 377–387.
[18] W.J. McCarter, T.M. Chrisp, G. Starrs, J. Blewett, Characterization and monitoring of cement based systems using intrinsic electrical property measurements, Cem. Concr. Res. 33 (2003) 197–206.
[19] P.W.J. Glover, M.J. Hole, J. Pous, A modified Archie's law for two conducting phases, Earth Planet. Sci. Lett. 180 (2000) 369–383.
[20] D.A. Robinson, S.P. Friedman, A method for measuring the solid particle permittivity or electrical conductivity of rocks, sediments, and granular materials, J. Geophys. Res. 108 (B2) (2003) (ECV 5–1 to 9).
[21] A.E. Bussian, Electrical conductance in a porous medium, Geophysics 48 (9) (1983) 1258–1268.
[22] P. Sheng, Effective medium theory of sedimentary rocks, Phy. Rev., B 41 (7) (1990) 4507– 4512.
[23] J. Bigalke, A study concerning the conductivity of porous rock, Phys. Chem. Earth 25 (2) (2000) 189–194.
[24] G.W. Milton, Bounds on the complex dielectric constant of a composite material, Appl. Phys. Lett. 37 (3) (1980) 300–302.
[25] J. Korringa, G.A. LaTorraca, Application of the Bergman–Milton theory of bounds to the permittivity of rocks, J. Appl. Phys. 60 (8) (1986) 2699–2976.
[26] E. Haslund, Dielectric dispersion of salt water saturated porous glass containing thin glass plates, Geophysics 61 (2) (1996) 722–734.
[27] K.S. Mendelson, M.H. Cohen, The effect of grain anisotropy on the electrical properties of sedimentary rocks, Geophysics 47 (2) (1984) 257–263.
[28] O.A.L. deLima, M.M. Sharma, A generalized Maxwell–Wagner theory for membrane polarization of shaly sands, Geophysics 57 (3) (1992) 431– 440.
[29] P. Gu, Z. Xu, P. Xie, J.J. Beaudoin, Application of A.C. impedance techniques in studies of porous cementitious materials — (I) influence of solid phase and pore solution on high frequency resistance, Cem. Concr. Res. 23 (1993) 531–540.
[30] B.J. Christensen, R.T. Coverdale, R.A. Olson, S.J. Ford, E.J. Garboczi, H.M. Jennings, T.O. Mason, Impedance spectroscopy of hydrating cement based materials: Measurement, interpretation and application, J. Am. Ceram. Soc. 77 (1994) 2789–2804.
[31] W.J. McCarter, G. Starrs, T.M. Chrisp, Electrical conductivity, diffusion, and permeability of portland cement-based mortars, Cem. Concr. Res. 30 (2000) 1395–1400.
[32] T.L. Chelidze, Y. Gueguen, C. Ruffet, Electrical spectroscopy of porous rocks: a review, Geophys. J. Int. 137 (1999) 16–34.
[33] P.N. Sen, Relation of certain geometric features to dielectric anomaly of rocks, Geophysics 46 (1981) 1714–1720.
[34] A.A. Garrouch, M.M. Sharma, The influence of clay content, salinity, stress, and wettability on the dielectric properties of brine saturated rocks: 10 Hz to 10 MHz, Geophysics 59 (6) (1994) 909–917.
[35] B. Nettelblad, G.A. Niklasson, The effects of salinity on low frequency dielectric dispersion in liquid-impregnated porous media, J. Phys., Condens. Matter 7 (1995) L619–L624.